

Classification

Physics Abstracts

61.30 — 64.70 — 62.20D

Oily streaks and focal conic domains in L_α lyotropic liquid crystals

P. Boltenhagen, O. Lavrentovich (*) and M. Kleman

Laboratoire de Physique des Solides (associé au CNRS), Bât. 510, Université de Paris-Sud, 91405 Orsay Cedex, France

(Received 11 April 1991, accepted 17 July 1991)

Abstract. — Observations with the polarizing microscope of defects in the lyotropic L_α (SmA) phase of the quasi-ternary system cetylpyridinium chloride/hexanol/brine give evidence that oily streaks are chains of focal conic domains. The chains are stable in the vicinity of the L_α - L_3 phase transition. Such a model of oily streaks was suggested long ago by G. Friedel but its existence was not confirmed unquestionably. We discuss the geometrical, topological and energetic properties of these structures and show that their stability depends on material constants, in particular, the saddle-splay rigidity \bar{K} , whose value can be estimated from the parameters of the oily streaks.

1. Introduction.

Oily streaks are the most common category of structural defects in layered (lamellar) liquid crystals, such as L_α , SmA, or N^* phases. They subdivide the ideal structure made of parallel flat layers, into domains and appear as long bands with a complex inner structure. Oily streaks were first observed by Lehmann [1] and discovered or rediscovered in various materials since (see e.g. [2-12]). Despite the long history of the question, the nature and the origin of oily streaks are still debated. To all appearance, the wealth of models involves the very nature of oily streaks and the dependence of their structure on the concrete values of the parameters of the medium [13].

Two main models are known. In the *disclination model* oily streaks are pairs of straight [10, 11] or undulating [12] disclinations; each pair of disclinations amounts to a dislocation, of possibly vanishing Burgers' vector. It seems that the model of undulating disclinations is closer to the real structure than the model of straight lines; as a matter of fact oily streaks possess a transversal striation [1-12], which is explained usually as an instability which relieves the elastic energy [10]. This model has certainly some range of validity.

However, this transversal striation may have another explanation within the scope of the *Friedel model* [2], which depicts oily streaks as chains of normal focal conic domains. These

(*) Also with Institute of Physics, Academy of Sciences of the Ukrainian SSR, pr. Nauki, 46, Kiev, 252028, Ukrainian SSR, U.S.S.R.

domains can nucleate from an edge dislocation [14], itself split into a disclination pair [15]. The smectic layers within each domain are folded around two conjugate focal lines, viz. an ellipse and hyperbola (in the case of « normal » focal conic domain), or two parabolae (in the limit case of the so-called parabolic focal domains [16, 17]). According to Friedel model [2], the striation is caused by the hyperbolae, which are perpendicular to the oily streak axis. In contrast with the disclination model, there is no adequate experimental confirmation of this model. The difficulties in the observations of oily streaks with clearly distinguished focal conics is caused by the possible large eccentricity of ellipses, as was already pointed out by Friedel [2]. In numerous observations [1-12] the periodicity of the transversal striation is indeed smaller than the width of the oily streak itself. This observation implies that the ellipses' eccentricity is large. On the other hand, as was discussed in detail in [18], if the ellipses have large eccentricities, they will be visible in the polarizing microscope only near the small part crossed by the hyperbola, and thus not recognizable as ellipses at all. Unfortunately, there is also a theoretical prediction that for typical smectic A liquid crystals with a curvature energy density

$$f = \frac{1}{2} K \left(\frac{1}{R_1} + \frac{1}{R_2} \right)^2 \quad (1)$$

(here R_1 and R_2 are two main radii of curvature, K is the bend constant), the elastic energy of focal conics is a decreasing function of eccentricity [17].

The above mentioned circumstances motivated us to look for the oily streaks as focal conics chains in systems where the lattest could be easily generated and possess small eccentricity. The possible candidate seems the lamellar phase L_α in the vicinity of the L_α - L_3 phase transition, where L_3 is the anomalous isotropic phase. In this region of the phase diagram the expected appearance of focal conic domains with small eccentricities should *a priori* relate to a factor which is particularly relevant to explain the stability of the L_α phase. Remember that the general expression for the bending elasticity (see for example [19]) reads :

$$f = \frac{1}{2} K \left(\frac{1}{R_1} + \frac{1}{R_2} \right)^2 + \bar{K} \frac{1}{R_1 R_2} \quad (2)$$

In this expression the first term is associated with the mean curvature and the second to the Gaussian curvature, with bend modulus K and \bar{K} , respectively. The \bar{K} term is generally disposed of, on the basis that it contributes only by a surface term to the total energy $\int f dv$. But it has to be taken into account in any modifications of the structure which involves a change in the topology of the layers, like for example the appearance of pores, passages, etc. According to Porte *et al.* [20], the phase transition from the L_α (where R_1 and R_2 tend to be infinitely large) to the L_3 phase (where R_1 and R_2 are of opposite signs) is mainly triggered by the saddle splay rigidity \bar{K} , which takes a large positive value in the L_3 phase. A large positive \bar{K} stabilizes indeed in the L_3 phase a large quantity of pores or handles, which are of negative Gaussian curvature, in the layers. Alternatively, in the L_α phase, since the transformation of the disclination pair to a chain of the focal conics requires the appearance of a negative Gaussian curvature, it seems natural to seek for oily streak focal conics in the vicinity of L_α - L_3 transition. The appearance of a correlated small eccentricity will be discussed in due course.

This paper will be divided as follows. After a description of the experimental results (optical observations) which definitely prove the presence of focal domains along the oily

streaks which exist in a certain domain of composition of the swollen lamellar system under study, we show experimentally that elementary oily streaks (this concept of « elementary » to be defined later) are defined by two invariants, a Burgers' vector b_x and an eccentricity e . The second invariant, as we show in a detailed calculation, is *material invariant* in samples of small enough thickness (compared to the width of the oily streak), and its experimental measure enables us to reach an estimate of the ratio \bar{K}/K . To the best of our knowledge, this is the first method ever proposed to measure the rigidity constant \bar{K} . Finally we complete this discussion of the oily streaks by stating the conditions under which we expect the other model to be valid.

2. Sample preparation.

We have investigated the L_a phase of the quasi-ternary system cetylpyridinium chloride (noted CpCl)/hexanol/brine (1 % by weight of NaCl). The weight fraction of brine was within the range 90 %-50 %. The surfactant (CpCl) and the cosurfactant (hexanol) were taken in weight proportion close to 1:1 for all samples. These concentrations correspond to the L_a phase in the vicinity of the L_a - L_3 phase transition. Samples poorer in hexanol i.e. in the vicinity of the L_a - L_1 phase transition (where L_1 is an isotropic phase), display completely different textures, which will be discussed in a forthcoming paper.

The samples for observations were prepared between glass slide and cover slip. To insure the homeotropic alignment of the lamellar phase the glasses were cleaned in chromic-sulfuric acid and rinsed with distilled water. Glasses were separated by two types of spaces: glass plates and mylar bands. In order to avoid the water evaporation and changes in the component concentrations, the samples were immediately sealed with a fast setting two-part epoxy resin. The procedure provides changes of the concentrations due to the evaporation less than 0.01 %. Observation was conducted by polarizing microscopy, at room temperature ($\approx 20^\circ\text{C}$).

3. Results.

3.1 TEXTURES OF OILY STREAKS.— The nucleation of oily streaks can be conveniently observed in flat capillaries in which the sample has been introduced by capillarity; these capillaries are subsequently sealed and let annealed at room temperature. Immediately after the introduction of the sample, one observes a set of very thin bright lines which are in the direction of the previous capillary flow. After a few hours, it is observed that these bright lines, which we believe are edge dislocations, gather together and form oily streaks of lateral extent comparable to the width of the capillary. However, since we do not have at our disposal a large enough set of capillaries of different thicknesses, we have made the quantitative studies on the previously described flat sealed cells.

Samples in flat sealed cells can be observed over a period of a few weeks. Initially disordered birefringent textures are observed. Within 1-2 hours or more the system relaxes by a very complex unfolding process towards a lower energy state with homeotropic texture and planar arrangement of layers. This texture is pseudo-isotropic and may be transformed into a brightly birefringent one by a slight downward pressure on cover slip. Oily streaks appear as long individual structured bands which subdivide the different homeotropic regions. Typical textures are shown in figures 1-4.

The main feature of the oily streaks observed between crossed polarizers is the presence of chains of ellipses; the minor axes of these ellipses are oriented along the long axes of oily streaks (Fig. 1). For sufficiently large ellipses (with size greater than the depth of field of the microscope, $\approx 10\ \mu\text{m}$ for the attachment we have used) it is possible by altering the position

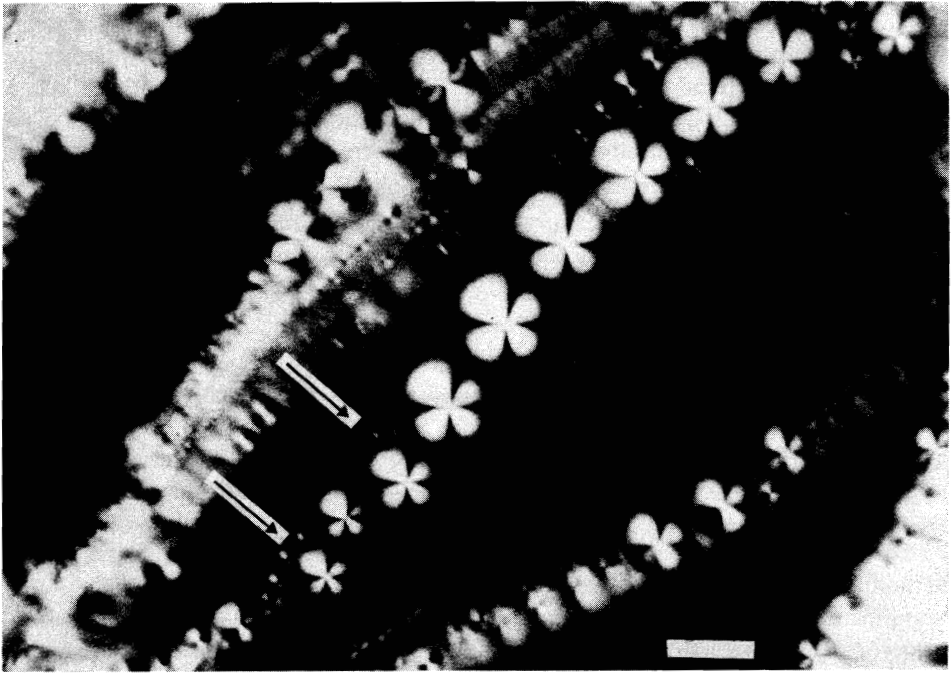


Fig. 1. — A typical array of the oily streaks with focal conic domains in the L_α phase of the system CpCl/hexanol/brine = 14.8/15.2/70. The width of the streak may be spanned by one or few (marked by arrows) domains. Crossed nicols, with vibration directions parallel to the edges of microphotograph. Sample thickness 130 μm . Bar : 50 μm .

of objective to trace another line, which lies in the vertical plane containing the major axis of the ellipse and passes the focus of ellipse. In textures this focus is crossed by four dark brushes. If the analyzer or polarizer is removed one can observe only two brushes emerging from the focus of ellipse.

The above described peculiarities are well-known optical properties of focal conic domains constructed on a set of conjugate ellipse and hyperbola [18]. The bilayers have the form of Dupin cyclides, which are the surfaces drawn normally to all straight lines joining any pair of points, one on the ellipse and the other one on hyperbola. In fact, these lines are the local optical axes of the system. In the ellipse plane they form a radial-like structure (with the center at the focus of ellipse) which gives 4 dark brushes of extinction in observations with crossed nicols.

The radial-like arrangement of the optical axes may be proved by the introduction of a quartz wedge (with its thin end first) into the 45° slot of the microscope. The interference color is raised for the two quadrants which are oriented along the direction of displacement of the wedge and reduced for the pair of quadrants in perpendicular position. Since the investigated system is optically uniaxial and positive, this means that the above mentioned radial-like distribution of the local optical axes lies in the ellipse plane.

The extinction bands of any given cross possess different lengths due to the eccentricity of the ellipse (Figs. 1-4). Often individual focal conic domains are observed ; they are embedded into a homeotropic matrix. In this case the structure is strictly axisymmetrical and the ellipse degenerates into a circle.

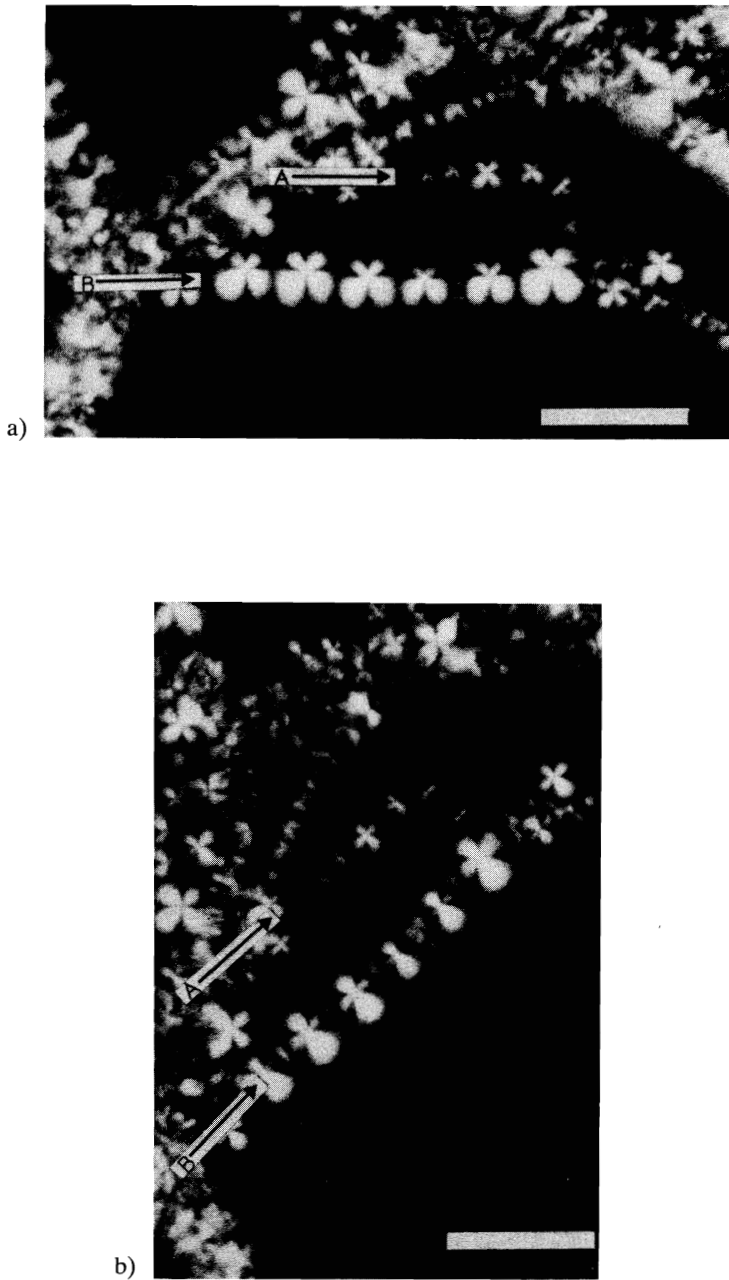


Fig. 2. — Oily streaks with focal conics of small eccentricity (A) and mean eccentricity (B). Crossed nicols with vibration directions along edges of photos. The gaps between ellipses are dark in both streaks, when they are oriented along vibration directions of nicols (a); for inclined orientation (b), streak B possesses bright gaps. L_α phase of CpCl/hexanol/brine = 15/15/70. Sample thickness 50 μm . Bar : 50 μm .

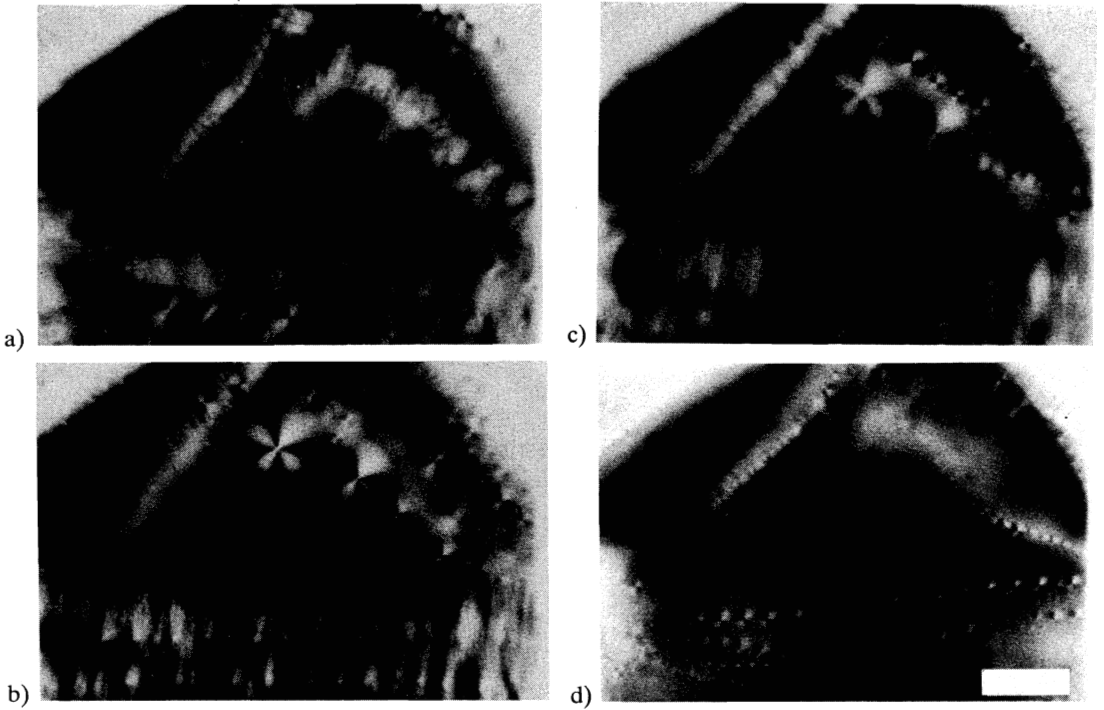


Fig. 3. — Oily streaks and individual focal domains located at different levels of a sample $620\ \mu\text{m}$ thick. a) Top array. Focused $200\ \mu\text{m}$ above centre of sample. b) Middle array. Focused at mid-height of sample. c) Bottom array. Focused $150\ \mu\text{m}$ below middle of sample ; d) Bottom array. Focused $250\ \mu\text{m}$ below middle of sample. Crossed nicols. $\text{CpCl}/\text{hexanol}/\text{brine} = 20/20/60$. Bar : $50\ \mu\text{m}$.

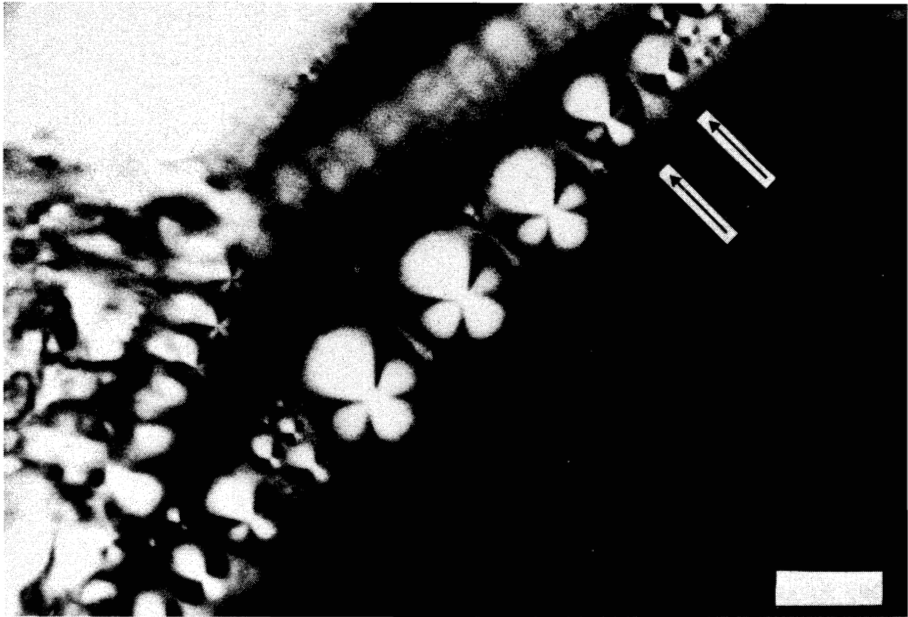


Fig. 4. — Streak which contains regions where ellipses do not span the whole width of the streak (some of them are marked by arrows). Crossed nicols, with directions parallel to the edges of microphotograph. $\text{CpCl}/\text{hexanol}/\text{brine} = 14.8/15.2/70$. Sample thickness $130\ \mu\text{m}$. Bar $50\ \mu\text{m}$.

Now let us consider the nature of the gaps between successive ellipses. If the axis of the oily streak lies along the direction of polarizer or analyzer these gaps are dark. For intermediate orientations the gaps exhibit some birefringence which depends on the eccentricity of the ellipses. This is demonstrated by figure 2, where two parallel chains A and B differ in the brightness of the gaps. For chain A with almost circular domains gaps are almost black for any orientation. In contrast, chain B possesses birefringent gaps for intermediate orientations between nicols. When the quartz wedge was introduced, the interference color of the gaps was raised for the oily streaks oriented normally to the direction of displacement of the wedge and a reduction of the retardation was observed for parallel orientation. This means that the local optical axis in the gaps is perpendicular to the oily streak axis.

3.2 PROPERTIES OF OILY STREAKS. — An important property of both oily streaks with focal conic chains and individual circular domains is their ability to be located at different levels of the sample thickness. Within one row of focal conics all ellipses lie in the same horizontal plane. However, by changing the microscope focus, one can easily distinguish in a thick sample numerous arrays of oily streaks with ellipses as well as individual domains which are located at different levels (Fig. 3).

We call « elementary » or « perfect » oily streak an oily streak whose constituted domains are all equal ; in such a case there are no other domains attached to the oily streak in the gaps. But this is not always the case : the ellipses which are formed along the same oily streak might possess different values of the major axes a and eccentricities e ; sometimes the large domains that constitute the oily streak might be replaced by a few smaller domain (see, e.g. Figs. 1 and 4). The major axis of the ellipses may be either greater (Figs. 1-3) or smaller (Fig. 4) than the oily streak width L , which is determined as the average width of the bright gaps between the ellipses. In the first case there is a relation between the eccentricity e of ellipses and the length of the major axis a : $a \cdot e \approx \text{const.}$ for the same oily streak, figure 5. In the second case this relation is violated, figure 5.

Here and farther on, the parameters of the ellipse (minor axis b , major axis a) are determined by the measurement of the maximal width of the focal conic domain along the streak axis and in its perpendicular direction. We used the microphotographs of textures obtained with crossed nicols. Also the elliptical shape of the domain base was independently checked up. It turned out that the boundary of the base satisfies the equation of an ellipse.

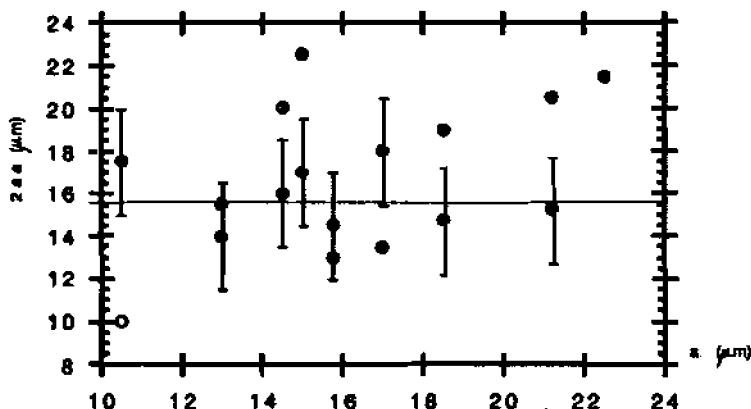
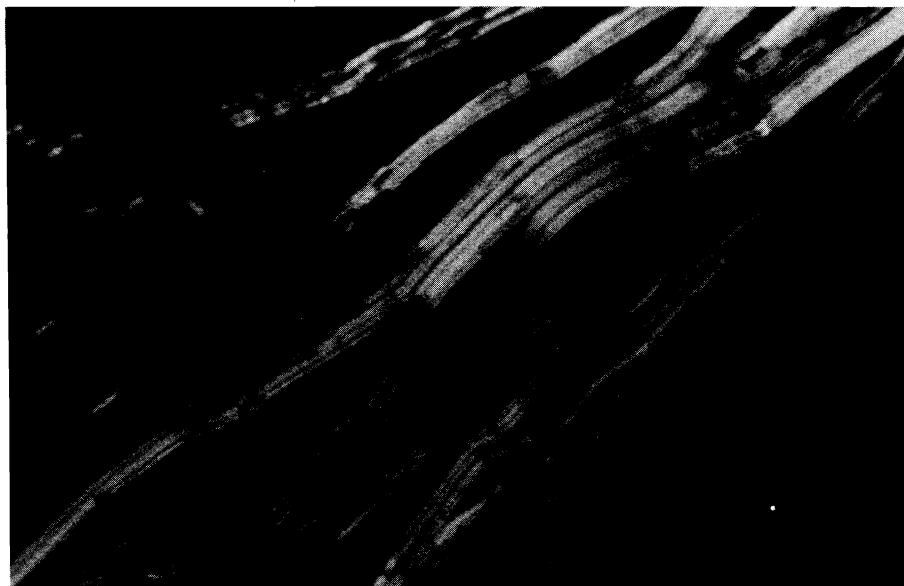
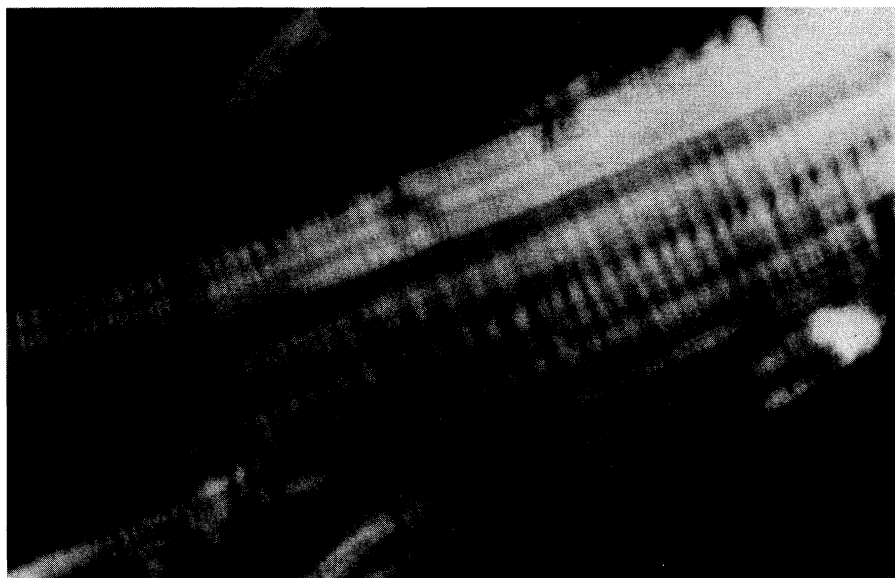


Fig. 5. — Dependencies of $2ae$ on the major axis a of the ellipses for two oily streaks : (●) streak width is completely covered by ellipses, $a \approx L$; (⊙) ellipses cover only part of streak width, $a < L$. CpCl/hexanol/brine = 20/20/60. Sample thickness $50 \mu\text{m}$.



a)



b)

Fig. 7. — Different structures of oily streaks in different regions of the phase diagram : a) Oily streaks as straight sets of line defects in the diluted L_α phase. CpCl/hexanol/brine = 6/6/88. Sample thickness 50 μm . b) Oily streaks as striated bands with almost undistinguished individual focal conic domains with high eccentricity in the L_α phase with comparatively low hexanol/CpCl ratio ; $\phi_{\text{hex}}/\phi_{\text{CpCl}} = 0.99$, $\phi_{\text{brine}} = 0.75$.

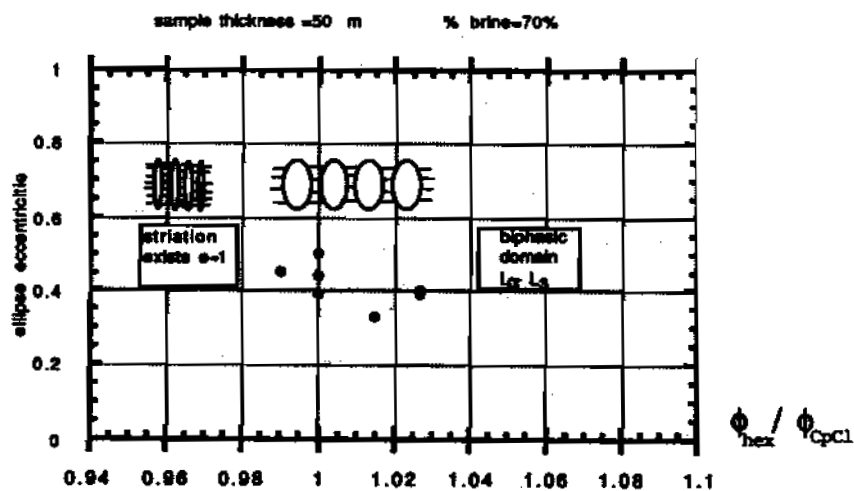


Fig. 8. — Ellipse eccentricities e vs. hexanol/CpCl ratio; $\phi_{\text{brine}} = 0.70$. Sample thickness 50 μ m.

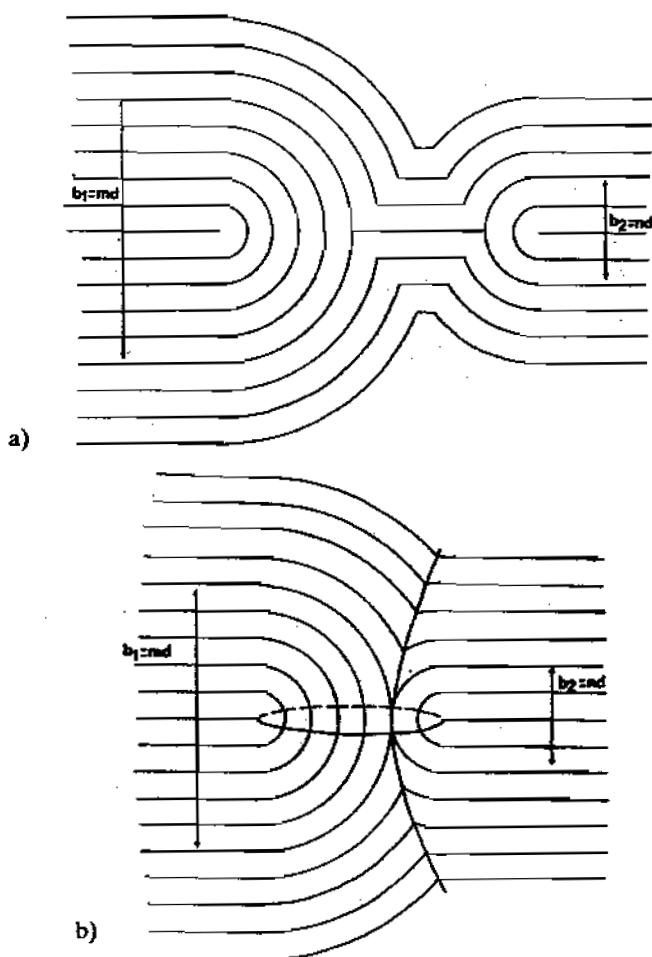


Fig. 9. — Two dislocations with Burgers vectors b_1 , and b_2 of opposite signs (a), which transform into a focal conic domain (b).

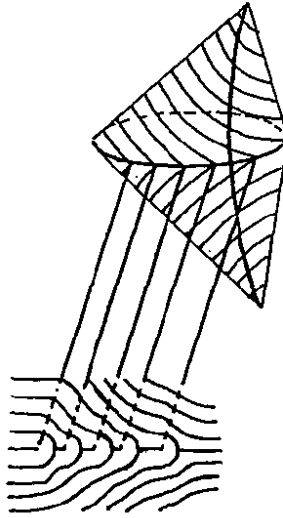


Fig. 10. — Appearance of edge dislocations in the region which surrounds a focal domain with non vanishing eccentricity.

parameters of this domain are determined by b_1 and b_2 : the major ellipse axis $a = \frac{b_1 + b_2}{2}$, the minor axis $b = \sqrt{b_1 b_2}$ and the eccentricity $e = (b_1 - b_2)/|b_1 + b_2|$ [22].

On the other hand, if one starts with a unique focal domain embedded in the homeotropic matrix, dislocations must emerge from this domain. The layers are inclined with respect to the ellipse plane at the cone boundary which limits a domain with nonzero eccentricity. As far as the ellipse plane is parallel to the sample boundaries (which is confirmed by experiment), these layers are also inclined with respect to the layers in the surrounding homeotropic regions. Thus, outside the domains, the resulting strains must be relaxed by edge dislocations, figure 10. It is easy to show that the total Burgers vector b_e of the dislocation set emitted by the focal domain obeys some topological rules and increases with the eccentricity e : $b_e = 2ae$. Circular domains do not emit dislocations.

Both processes mentioned above lead to the same key elements of the oily streak structure, which proceeds essentially from the topology of a set of parallel (or almost parallel) dislocations, dissociated into a disclination set which is in turn more or less unstable with respect to the formation of focal conic domains, figure 11. This model is confirmed by experiment. Consequently, in accordance with the model, the gaps between focal conic domains must be filled with sets of parallel disclinations (or edge dislocations). It means that the local optical axis in gaps is oriented in plane of oily streak and normally to the axis of the streak. The latter is undoubtedly observed in experiment.

Obviously m elementary dislocations with elementary Burgers vector $b = +d$ and n elementary edge dislocations of opposite sign, $b = -d$, may be dissociated in different manners in disclination pairs. Furthermore, the number of these pairs may be different for different parts along the oily streak without the violation of the conservation law $m - n = \text{const}$. As a result, these dislocation pairs will transform into focal conics with different sizes and eccentricities.

Of course, in any case the total Burgers vector of the oily streak must be constant: when the streaks form a network with nodes, the total Burgers vector of the streaks entering and leaving a node must be equal, according to Kirchoff's network relationship [10].

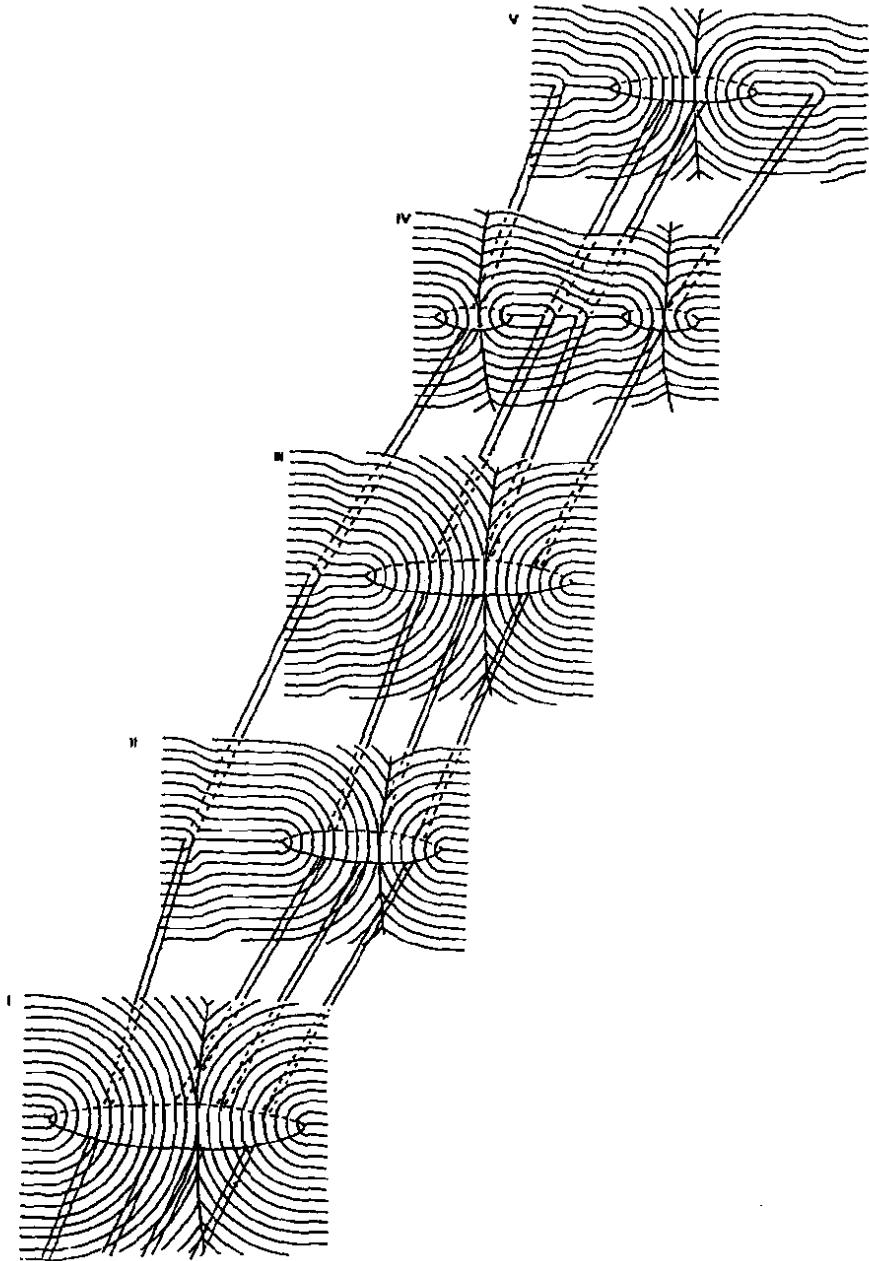


Fig. 11. — Scheme of the general structure of an oily streak. 5 vertical cross-sections with distribution of layers as well as the sets of ellipses and edge dislocations in the plane of streak are shown. The corresponding geometrical parameters are indicated in table I.

For the particular case of an individual oily streak with a width L completely covered by ellipses, the conservation law of the streak Burgers vector b_e takes the simple form

$$b_e = 2 a_i e_i = \text{const.} \quad (3)$$

Here a_i and e_i are the parameters of any ellipse that is involved in the streak structure. This

result is confirmed by experimental situation, figure 5. It is remarkable that it is not necessary to keep a_i and e_i constant simultaneously along the streak. Thus, during the unfolding of the initial strongly deformed structure, the different ellipses with different a_i, e_i , which satisfy the condition $a_i e_i = \text{const.}$, may appear. Obviously, the probability of the appearance of certain a_i, e_i is governed by the growth conditions as well as by the elastic energy as a function of a_i and e_i .

The connection between b_e and e_i is clearly illustrated in figure 2. It is natural to assume that the brightness of the gaps between the ellipses must increase with b_e . Due to the conservation law, if $e_i \rightarrow 0$, then for the corresponding oily streak $b_e \rightarrow 0$ also and the gaps are dark for any position of the streak between crossed nicols, because of the low birefringence. With increasing e_i and, consequently, b_e , the brightness of the gaps increases. This is demonstrated in figure 2 by the comparison of two oily streaks, A and B, where A has a low-eccentricity and B contains ellipses with large $e_i(0.4-0.5)$. It seems important to note that e_i for streak A is small, but non-vanishing : focal domains tend to be oriented along one axis, hence, there is the dislocation set along this axis, with nonzero line tension. Focal domains with $e_i = 0$ do not emit dislocations and, as a result, do not form chains.

Using (3), one can calculate the total Burgers vector of the individual streaks, by measuring the parameters of ellipses. For samples with thicknesses 50-600 μm , typical values are 10-20 μm , which corresponds to $\sim 10^3$ bilayers for the systems investigated.

In the general case, when there are N ellipses with some a_i, e_i arranged along the same cross-section of the oily streak and M dislocations with Burgers vector b_j , that cross the same normal plane but pass over the focal domains, the conservation law takes the form

$$b_e = 2 \sum_{i=1}^N a_i e_i + \sum_{j=1}^M b_j = \text{const.} \quad (4)$$

This law is illustrated in figure 11 and table I.

Table I. — Geometrical parameters of the oily streak depicted in figure 11. The total Burgers vector of the oily streak conserves for all the cross-sections of structure despite the differences in the number of elementary dislocations and differences in the geometry of the focal conic domains (major axis a and eccentricity e). All parameters are presented in the units of interlayer distance of figure 11.

Cross section	Dislocations, Burgers vectors	Focal conic domains				Total Burgers vector of oily streak
		a_e	b_e	e	$\sum_{i=1}^N 2 a_i e_i$	
N_0	$\sum_{j=1}^M b_j$	a_e	b_e	e	$\sum_{i=1}^N 2 a_i e_i$	$b_e = \sum_{j=1}^M b_j + 2 \sum_{i=1}^N a_i e_i$
I	—	24	$\sqrt{560}$	1/6	8	$8 = 0 + 8$
II	1 + 1	15	$\sqrt{216}$	1/5	6	$8 = 2 + 6$
III	1 + 1	19	$\sqrt{352}$	3/19	6	$8 = 2 + 6$
IV	1 + 1 + 1 + 1	7(*2)	$\sqrt{48} (*2)$	1/7(*2)	2 + 2	$8 = 4 + 4$
V	1 + 1 + 1 + 1	14	$\sqrt{432}$	1/7	4	$8 = 4 + 4$

4.2 TOPOLOGY OF THE OILY STREAKS. — It is necessary to stress the significant topological differences between the oily streaks which are made of focal domains, and the oily streaks which are made of straight [11] or undulating [12] line defects (Fig. 12). This difference results in different values of the Gaussian curvature $(R_1 R_2)^{-1}$.

In the disclination model [12], the striation of the streaks is caused by undulations of the disclination pair. The radii R_1 and R_2 of the layer curvatures are finite. Nevertheless, the average Gaussian curvature $(R_1 R_2)^{-1}$ of this structure is zero: R_2 , which determines the curvature in the plane of streak, changes sign with the period of the undulation along the streak axis. This result is the direct consequence of the Gauss-Bonnet theorem which may be illustrated by the fact that a simple deformation of the undulated disclination pair turns it into a (topologically equivalent) straight pair. For the latter R_2 is infinitely large and $(R_1 R_2)^{-1} = 0$ for all regions of the streak.

Alternatively, in the Friedel model, the formation of the focal conic domains requires changes in the layer topology. Now, within one domain, R_1 and R_2 always possess different

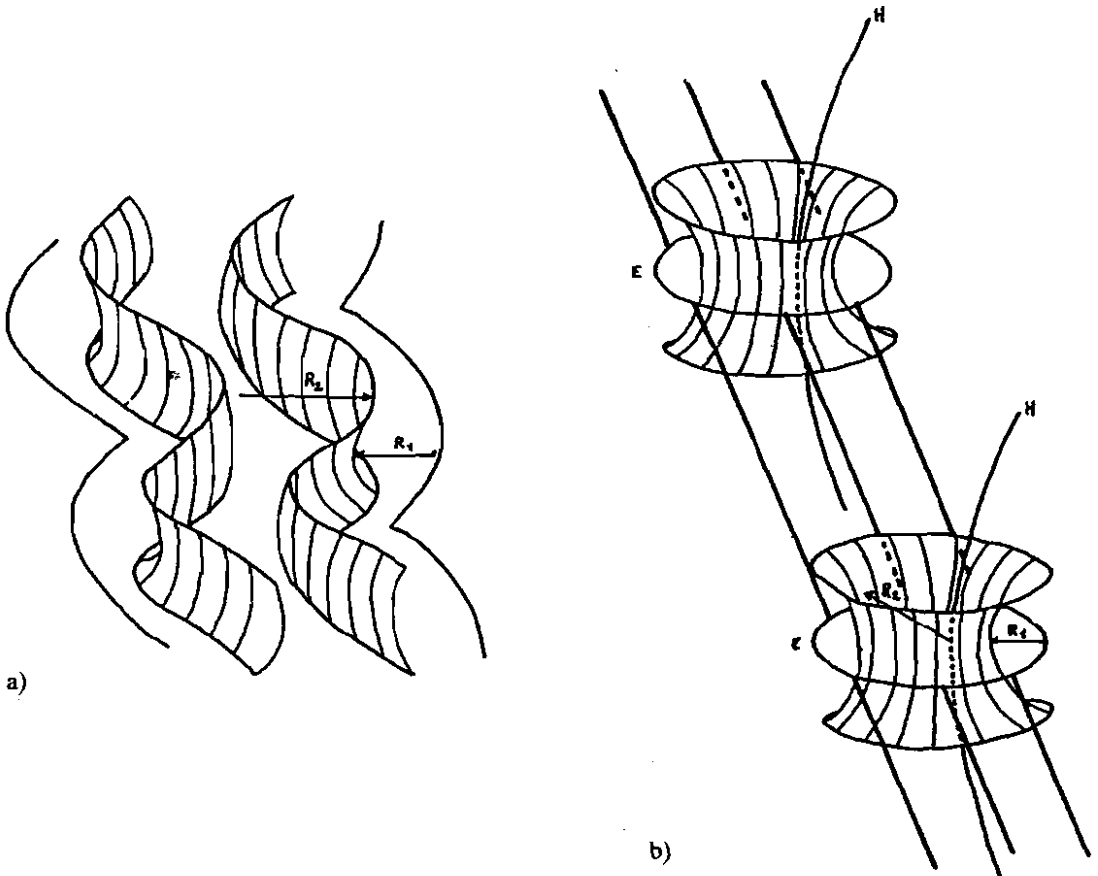


Fig. 12. — Topological differences in different models of oily streaks : a) The Schneider-Webb model, the average Gaussian curvature is zero ; b) Friedel model, $(R_1 R_2)^{-1} = 0$ only within the gaps between domains.

signs. Thus, for those regions of streak which are occupied by domains, $(R_1 R_2)^{-1} < 0$. Of course $(R_1 R_2)^{-1} = 0$ in the gaps between domains.

These topological differences yield different oily streak energies for materials with non-zero \bar{K} . As already stated (see e.g. [19]), a positive \bar{K} favours saddle-splay curvature of the layers (precisely the case of the focal domains), while a negative \bar{K} favours spherical-like curvatures (see e.g. [19]). This question is discussed below for focal conics and oily streaks in L_α phases with $\bar{K} \neq 0$.

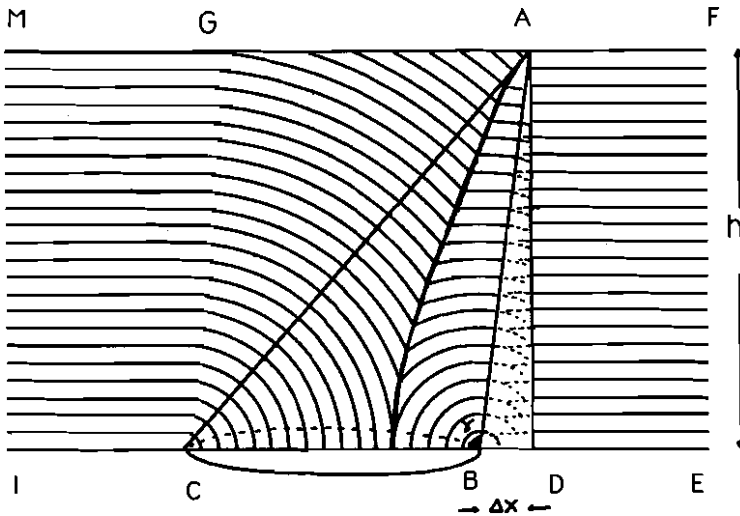


Fig. 13. — Vertical cross-section of a focal domain (ABC region) and of two surrounding homeotropical regions ADEF and CGHI by a plane which contains the major axis of the ellipse. In the transient regions there is violation of layer equidistance (ABD).

4.3 ENERGIES OF FOCAL DOMAINS AND OILY STREAKS. — The transformation of the set of edge dislocations into chains of focal conics or an undulating pair of disclinations should depend on the geometrical parameters, topological properties, as well as on the elastic modulus of the L_α phase. In the general case, three constants are involved in the expression for the free energy density f associated with the bulk elastic distortions of L_α phases :

$$f = f_K + f_R + f_B = \frac{1}{2} K \left(\frac{1}{R_1} + \frac{1}{R_2} \right)^2 + \frac{\bar{K}}{R_1 R_2} + \frac{1}{2} B \epsilon^2, \tag{5}$$

where the first two terms describe the curvature of layers and the third one describes the energy of layer displacement, measured along its normal : ϵ is the relative layer thickness variation.

The curvature energy of an isolated focal conic domain for a material with $\bar{K} \neq 0$ may be calculated using Kléman's analytical description [17], which employs the Darboux's method of local axes at each point of each layer. The infinitesimal area of the surface of a layer in rectangular curvilinear coordinates (u, v) is given by [17]:

$$d\Sigma = AB \, du \, dv,$$

where $u = \text{const.}$ and $v = \text{const.}$ are the lines of curvature of layer. For the geometry of a focal domain with $R_1 R_2 < 0$, $R_1 < 0$, $R_2 > 0$, the coefficients A and B take the form [17]

$$A = \frac{b\sigma_2}{\sigma_2 - \sigma_1}; \quad B = \frac{b\sigma_1}{\sigma_1 - \sigma_2}, \quad (6)$$

$$\sigma_1 = 1/R_1 = 1/(ea \cos v - z), \quad \sigma_2 = 1/R_2 = 1/(achu - z),$$

where z is measured along any normal to the layers and varies in the range $[-c, +\infty)$, with $c = a/e$.

The calculation of the focal domain energy W , therefore, involves the calculation of the integral

$$W = \int (f_K + f_R) AB \, du \, dv \, dz \quad (7)$$

over the volume of two semi-infinite cylinders (oblique in the general case) parallel to the asymptotes of the hyperbola and whose base is the ellipse. Following [17], by using (2), (6) and (7), one obtains:

— an exact solution for $e = 0$

$$W = 2 \pi^2 Ka \left(\ln \frac{2a}{r_c} - 2 - x \right), \quad (8)$$

— an approximate solution for small e (when E is almost a circle):

$$W = 2 \pi K(1 - e^2) a \mathcal{K}(e^2) \left[2 \ln \frac{a}{r_c} + 1 - 2x \right] + K(1 - e^2) a \pi^2 (2 \ln 2 - 5), \quad (9)$$

— and, in the general case, for all possible $e \neq 1$,

$$W = 4 \pi K(1 - e^2) a \mathcal{K}(e^2) \left[\ln \frac{a}{r_c} - 2 - x \right] + K(1 - e^2) a \int \frac{\ln |e \cos v - \cosh u|}{\cosh u - e \cos v} \, du \, dv. \quad (10)$$

Here $\mathcal{K}(e^2)$ is the complete elliptic function of the first kind ($\mathcal{K}(0) = \pi/2$) and is a very quickly increasing function of e^2 ; $x = \bar{K}/K$; r_c is a core radius along the ellipse and the hyperbola and may be taken of the order of the smectic coherence length. The energies of the ellipse and hyperbola cores are difficult to calculate, since these are the singular regions. They scale as $\sim \xi KL_E$, where ξ is some geometrical constant, and L_E is the ellipse length $L_E = 4 a \mathcal{K}(e^2)$ [17]. For the sake of simplicity we will neglect this term.

The chains of focal domains arise along the set of edge dislocations when $W < W_d$, where the energy W_d of dislocations with length b may be estimated as [22] $\sqrt{KB} b_e b$.

Thus, focal conics are energetically preferable for sufficiently large Burgers vectors

$$b_e \gg q\Lambda, \quad (11)$$

where $\Lambda = \sqrt{K/B}$ and the numerical constant q depends both on x and e ; for small e

$$q \approx 2 \pi^2 (1 - e^2)^{\frac{1}{2}} \left[\ln \frac{2a}{r_c} - 2 - x \right]. \quad (12)$$

The dependency $q(x)$ is indeed what we expect: positive x favours the appearance of the focal domains in the streaks. On the other hand, q is a decreasing function of e , due to the decreasing of $(1 - e^2) \mathcal{K}(e^2)$ with e [17]. This contradicts the experimental observation of ellipses with small $e \sim 0.1-0.5$ in oily streaks. Low values of e must therefore be stabilized by some external factor [19]. For discussed situation the stabilization is caused by conservation law, as well as by nonzero values of modulus B . For thermotropic systems the anchoring energy may also be important [23]. Let us discuss this question in more detail.

By definition, an oily streak separates the homeotropic regions with horizontal layer packing. As was pointed out above, the inclination of the layers on the focal domain boundary with respect to the horizontal plane creates a dislocation set along the direction of the minor ellipse axis. However, for $e \neq 0$ this inclination also leads to the singularities in the plane, which contains major axis, figure 12, region ABD. The layers can cross smoothly from the homeotropic region to domain region ABC without violating of the equidistance only when the angle γ between the base CB and the conical boundary of domain (line AB) is smaller than or equal to $\pi/2$. This smooth crossing is possible only for circular domains in thick samples or for elliptical domains in samples with thickness $h \leq a(1 - e^2)/e$; the last condition is equivalent to $\gamma \leq \pi/2$ and restricts the possible values of the eccentricity.

In the general case, however, $\gamma > \pi/2$ and the violation of the layer thickness in ABD region yields a nonzero compressibility term $W_B \sim \frac{1}{2} B \epsilon^2 V$, where $\epsilon \sim (\gamma - \pi/2)^2$, $V \sim hb \Delta X$, $\Delta X \sim (he/\sqrt{1 - e^2} - a) > 0$, ΔX is the length of line BD. One gets that this term increases with e and B :

$$W_B = \frac{\beta B a^5 b}{h^3} \left(\frac{eh}{a(1 - e^2)^{\frac{1}{2}}} - 1 \right)^5, \tag{13}$$

where β is some geometrical constant, $\beta \sim 1$.

One can estimate the total energy of oily streak per unit length as $(W + W_B)/b$:

$$\omega = 2 \pi^2 K (1 - e^2)^{\frac{1}{2}} \left[\ln \frac{2a}{r_c} - 2 - x \right] + \frac{\beta B a^5}{h^3} \left(\frac{eh}{a(1 - e^2)^{\frac{1}{2}}} - 1 \right)^5, \tag{14}$$

where the elliptic function $K(e^2) \approx \frac{\pi}{2} \left(1 + \frac{e^4}{4} + \dots \right)$ in expression (9) is replaced by $\frac{\pi}{2}$.

To ascertain the values of e which correspond to a stable state of oily streak it is necessary to minimize (14) with respect to e and a , taking into account the conservation law (3) for the Burgers vector b_s .

The problem is difficult to solve analytically without additional simplification. Let us start with the limit case.

a) $B = 0$. It is easy to find that in this case, a small value of the eccentricity results from a large positive \bar{K} :

$$e^2 = \frac{K}{\bar{K} + K \left(3 - \ln \frac{b_s}{r_c e} \right)}. \tag{15}$$

This solution satisfies the stability conditions $\frac{\partial^2 \omega}{\partial e^2} > 0$ and $\left(\frac{\partial^2 \omega}{\partial a \partial e} \right)^2 - \frac{\partial^2 \omega}{\partial a^2} \frac{\partial^2 \omega}{\partial e^2} > 0$ and corresponds thus to the minima of ω . However, in this case $\frac{\partial^2 \omega}{\partial a^2} < 0$.

b) $B \neq 0$. i) If the sample is sufficiently thin, $eh \ll b$, we are again in the situation of case a) and e is determined by ratio \bar{K}/K in accordance with (15); ii) For thick samples, when $he \gg b$, the minimization yields the following equilibrium value of e :

$$e^3 \approx \frac{2 \pi^2 K}{5 \beta^2 B h^2} \left[\ln \frac{b_\varepsilon}{er_c} - 3 - x + \frac{1}{e^2} \right]. \quad (16)$$

As before, $\frac{\partial^2 \omega}{\partial e^2} > 0$, $\left(\frac{\partial^2 \omega}{\partial a \partial e} \right)^2 - \frac{\partial^2 \omega}{\partial a^2} \frac{\partial^2 \omega}{\partial e^2} > 0$ and $\frac{\partial^2 \omega}{\partial a^2} < 0$.

An analysis of (16) shows that a possible decrease of e might originate in one of the following causes: (I) the increase of the sample thickness h ; (II) the decrease of the penetration length $\Lambda = \sqrt{K/B}$ and (III) the increase of the ratio $x = \bar{K}/K$.

In particular

$$e^5 \sim K/Bh^2, \quad \text{if} \quad \left(\ln \frac{b_\varepsilon}{er_c} - 3 - \frac{\bar{K}}{K} \right) \ll e^{-2}. \quad (17)$$

As it follows from (15)-(17) there are at least three factors that favour the smallness of the eccentricities observed i.e. the increases of \bar{K}/K , B , and h . The decrease of e with h for thick samples ($h > b_\varepsilon$) is qualitatively confirmed by the experimental data of figure 6. In order to separate the data for oily streaks with different values of Burgers vector, the sets of points in figure 6 are marked by different symbols for different b_ε .

Now, let us come back to the experimental observation that oily streaks with focal conics are replaced (a) by straight streaks without visible striation for highly diluted L_α phase or (b) by striated streaks without visible focal conics for low concentration of hexanol, figure 7. Naturally, in all the cases examined $h \approx \text{const.}$ and the observed peculiarities correspond to the changes in \bar{K}/K and B values with brine and hexanol concentrations.

In order to trace the behaviour of \bar{K}/K and B under a change of concentration, let us briefly recall the nature of the swollen L_α phase.

4.4 OILY STREAKS AND PHASE DIAGRAM. — As was shown by light scattering experiments [24] for CpCl/hexanol/brine system, at a given hexanol to CpCl ratio, the lamellar phase expands unidimensionally so that $d = d_0/(1 - \phi_{\text{brine}})$, where d_0 is the thickness of the « dry » lamella ($d_0 \approx 27 \text{ \AA}$) and ϕ_{brine} is the brine volume fraction. For a diluted system, $\phi_{\text{brine}} = (0.7 - 0.98)$, d is much greater than d_0 . Nevertheless, despite the large separating distance, lamellae keep smectic order. The only repulsive interaction which is likely to be responsible for the stability of the structure may be the long-range « steric interaction » [25]. The latter arises due to the steric hindrance of thermal fluctuations of the adjacent layers. The large repeat distance d , obviously, corresponds to very low elastic constants.

As was shown by Helfrich [27] within the scope of the « steric interaction » model, the layer compressibility modulus B scales as

$$B \approx \frac{5(k_B T)^2}{\kappa_c d^3},$$

where $\kappa_c = Kd$ is the curvature modulus of the lamellae. Therefore, $B \sim (1 - \phi_{\text{brine}})^3$ and $K \sim (1 - \phi_{\text{brine}})$. Since the energy W_d of the dislocation set scales like \sqrt{KB} , and the energy of focal conic chains scales like K , one can expect that for highly diluted L_α phase the condition (11) is not satisfied. It means that, in systems with small B , oily streaks may be represented by sets of edge dislocations rather than by focal conic chains. This result can explain why it was impossible to find oily streaks with visible focal domains or striations in samples under the increasing of ϕ_{brine} above 0.88 and keeping constant hexanol to CpCl ratio, $\phi_{\text{hex}}/\phi_{\text{CpCl}} = 1$. As was already pointed out in section 3.2, oily streaks for $\phi_{\text{brine}} > 0.88$ look like straight bands (Fig. 7a).

Now, let us discuss the behaviour of oily streaks for the same $\phi_{\text{brine}} < 0.88$, but for different $\phi_{\text{hex}}/\phi_{\text{CpCl}}$ ratios. As far as $\phi_{\text{brine}} < 0.88$ B is not too small, one expects that focal conic chains would show up rather than dislocation sets. With fixed ϕ_{brine} , as was argued in [20], the increase of $\phi_{\text{hex}}/\phi_{\text{CpCl}}$ leads to the increase of \bar{K} from negative values up to positive ones. Therefore, in accordance with (16), the ellipses' eccentricity tends to decrease. It is natural to assume that for comparatively low values of $\phi_{\text{hex}}/\phi_{\text{CpCl}} \approx 0.99$ the striated oily streaks are formed by chains of domains with large eccentricity, $e \rightarrow 1$. Such domains, as was stressed in the introduction, are however extremely hard to distinguish in the oily streak structure. In the vicinity of the L_α - L_3 phase transition, with $\phi_{\text{hex}}/\phi_{\text{CpCl}} \approx 1.027$, e is smaller, $e \sim 0.4$ at least (Fig. 8). Using (15), one can estimate the ratio \bar{K}/K for different parts of the L_α - L_3 pretransition region. With $b_e \approx 10 \mu\text{m}$, $r_c \sim d \sim 150 \text{ \AA}$ one obtains $\bar{K}/K \sim 10$ for $\phi_{\text{hex}}/\phi_{\text{CpCl}} = 1.027$ and $\bar{K}/K \sim 6$ for $\phi_{\text{hex}}/\phi_{\text{CpCl}} = 0.99$.

5. Conclusion.

We have experimentally observed and theoretically described the oily streaks in the lyotropic L_α phase close to the L_α - L_3 phase boundary. The textural observations give evidence that the oily streaks are the chains of focal conic domains. Key element of the oily streak structure is a set of dislocations, dissociated into a disclination set, which is in turn unstable with respect to the formation of focal conic domains. The conservation law of the oily streak Burgers vector b_e poses a restriction ($ae = \text{const.}$) on the geometrical parameters of domains, viz., the ellipse eccentricity e and the major axis a . The equilibrium value of e is determined by the ratio of the saddle-splay \bar{K} to the bend K moduli and thus is material invariant. Its experimental measure has enabled us to reach an estimate of \bar{K}/K ratio.

References

- [1] LEHMAN O., Flüssige Kristalle. Leipzig (1904).
- [2] FRIEDEL G., *Ann. Phys. France* 18 (1922) 273.
- [3] STEERS M., KLÉMAN M. and WILLIAMS C. E., *J. Phys. France* 35 (1974) L21.
- [4] RAULT J., *C.R. Acad. Sci. Paris* 280B (1975) 417.
- [5] CHISTYAKOV I. Gr., *Sov. Phys. Crystallogr.* 7 (1963) 619.
- [6] GERRITSMAN C. J. and VAN ZANTEN P., *Liquid Cryst.* 3, Eds. G. H. Brown and M. M. Labes (New York: Gordon and Breach, 1976), p. 751.
- [7] NAGEOTTE J., *Morphologie des gels lipoides* (Hermann and Cie, Paris, 1936).
- [8] SAUPE A., *J. Colloid. Interface Sci.* 58 (1977) 549.
- [9] CANDAU F., BALLEST F., DEBAUVAIS F. and WITTMANN J.-C., *J. Colloid Interface Sci.* 87 (1982) 356.

- [10] KLÉMAN M., COLLIEX C. and VEYSSIÉ M., *Advances in Chemistry Series*, n° 152, Ed. Friberg S. (Amer. Chem. Soc., Washington, D. C., 1976), p. 71.
- [11] ASHER S. A. and PERSHAN D. S., *Biophys. J.* **27** (1979) 393.
- [12] SCHNEIDER M. B. and WEBB W. W., *J. Phys. France* **45** (1984) 273.
- [13] KURIK M. V. and LAVRETOVICH O. D., *Uspekhi Fiz. Nauk* **154** (1989) 381 ; *Sov. Phys. Usp.* **31** (1988) 196.
- [14] WILLIAMS C. and KLÉMAN M., *J. Phys.* **36** (1975) C1-315.
- [15] RAULT J., *Philos. Mag.* **34** (1976) 753.
- [16] ROSENBLATT Ch. S., PINDAK R., CLARK N. A. and MEYER R. B., *J. Phys. France* **38** (1977) 1105.
- [17] KLÉMAN M., *J. Phys. France* **38** (1977) 1511.
- [18] HARTSHORNE N. H. and STUART A., *Crystals and the Polarizing Microscope* (Edward Arnold, London, 1970).
- [19] KLÉMAN M., *Rep. Prog. Phys.* **52** (1989) 555.
- [20] PORTE G., APPELL J., BASSEREAU P. and MARIGNAN J., *J. Phys. France* **50** (1989) 1335.
- [21] KLÉMAN M. and FRIEDEL J., *J. Phys. France* **30** (1969) C4-43.
- [22] KLÉMAN M., *Points, Lines and Walls in Anisotropic Fluids and Ordered Media* (Wiley, Chichester, 1983).
- [23] LAVRETOVICH O. D., *Zh. Eksp. Teor. Fiz.* **91** (1986) 1666 ; *Sov. Phys. JETP* **64** (1986) 984.
- [24] GOMATI R., APPELL J., BASSEREAU P., MARIGNAN J. and PORTE G., *J. Phys. Chem.* **91** (1987) 6203.
- [25] DE GENNES P. G., *J. Chem. Phys.* **48** (1968) 2257.
- [26] DI MEGLIO J. M., DVOLAITSKY M. and TAUPIN C., *J. Phys. Chem.* **87** (1985) 871.
- [27] HELFRICH W., *Z. Naturforsch.* **33a** (1978) 305.